ELSEVIER

Chemical Engineering Journal 78 (2000) 69–79

Chemical Engineering Journal

www.elsevier.com/locate/cej

Application of heat interchange systems to enhance the performance of ammonia reactors

M.E.E. Abashar*

Reaction and Fluidization Engineering Group (RFEG), Chemical Engineering Department, University of Durban Westville, Private Bag X54001, Durban, South Africa

Received 5 February 1999; received in revised form 30 October 1999; accepted 4 December 1999

Abstract

A rigorous heterogeneous model for adiabatic ammonia reactors is used to explore the application of internal heat exchange theory to cross the adiabatic reaction equilibrium values and to improve the conversion in ammonia reactors. The mathematical model is developed for adiabatic ammonia converters and the resulting two-point boundary value differential equation for the catalyst particles is solved using the orthogonal collocation method. Two simple configurations of reactors with heat interchangers are implemented. An industrial ammonia reactor having three adiabatic beds with Montecatini Edison catalyst and interstage cooling is used as the basis for comparison. The comparison shows that an increase of 13.37% of the overall ammonia conversion is possible. The results presented in this study reveal the potential application of energy optimization and integration in the ammonia industry.

Keywords: Heterogeneous model; Ammonia reactors; Energy optimization

1. Introduction

Ammonia is produced by an exothermic reversible reaction of hydrogen with nitrogen. The chemical reaction shares the general problem of exothermic reversible reactions that is the conversion is limited by the thermodynamic equilibrium. For exothermic reversible reactions, the increase of temperature increases the rate of the reaction but decreasing the equilibrium conversion. The equilibrium conversion is the maximum conversion that can be achieved. Different approaches have been considered to overcome thermodynamic limits on the maximum attainable conversion of reversible reactions. Membrane reactors combining reaction and separation of products are known as versatile devices for equilibrium shifting [1,2]. Despite the significant advantages of membrane reactors the technology is still limited to certain kinds of reactions and is not commercially utilized. In a recent study [3], it has been shown that a considerable increase in the conversion of reversible reactions is possible for adiabatic reactor systems by crossing the adiabatic reaction equilibrium values using internal heat exchange. Interstage cooling is also widely employed to improve the conversion of exothermic reversible reactions [4–6]. Many optimization studies have been reported in the literature which addressed the problem of maximizing the conversion by optimizing the temperature profile along the reactor length [7].

In the ammonia industry, conversion is usually improved by shifting the reaction from the thermodynamic equilibrium through: direct quenching of reacting gases with fresh synthesis gas (e.g. the Pullmann–Kellogg and Chemico converters), quenching of the reaction mixture by external cooling (e.g. the Montecatini Edison converters) and heat exchange with reacting gases (e.g. the TVA converters) [8]. Despite the efforts made to achieve the best temperature profile, conversion in ammonia reactors is still relatively low.

The purpose of this preliminary study is to explore the potential application of internal heat exchange to optimize the conversion of adiabatic ammonia converters. The different temperature states in adiabatic ammonia reactors are used to optimize the energy usage and to enhance the conversion. Mathematical modelling is involved as a powerful tool for simulation and optimization. The major difference between this study and the earlier ones is that the ammonia reactor is converted into systems consisting of reactors and heat interchangers and each system is assumed adiabatic overall, i.e. no external means is used to heat or to cool the reaction mixture. Rigorous optimization analysis and the cost factors are not included in this preliminary study.

* Tel.: +27-31-2044483/187; fax: +27-31-2044021.
E-mail address: mabashar@pixie.udw.ac.za (M.E.E. Abashar)

1385-8947/00/$ – see front matter
PII: S1385-8947(99)00175-8

2. Rate expression

The intrinsic modified form of the Temkin rate expression [9] is used in the developed model, as follows:

$$R_{NH_3} = k_2 \left[K_a^2 f_{N_2} \left(\frac{f_{H_2}^3}{f_{NH_3}^2} \right)^{\alpha} - \left(\frac{f_{NH_3}^2}{f_{H_2}^3} \right)^{1-\alpha} \right] \quad (1)$$

where R_{NH_3} is the reaction rate in kmol of NH_3/(h m^3 of catalyst bed), k_2 the velocity constant for the reverse reaction in kmol/(h m^3), and K_a the equilibrium constant of the reaction

$$\tfrac{1}{2}N_2 + \tfrac{3}{2}H_2 \rightleftarrows NH_3 \quad (2)$$

where f_{N_2}, f_{H_2}, and f_{NH_3} are the fugacities of nitrogen, hydrogen, and ammonia, respectively, and α is a constant. The velocity constant, k_2, is estimated by the Arrhenius relation of the form [10]:

$$k_2 = k_{20} \exp\left(\frac{-E_2}{R_G T} \right) \quad (3)$$

The respective values for the Montecatini Edison catalyst are α=0.55, E_2=1.635×10^8 J/kmol, and $\log k_{20}$=14.7102, and R_G is the universal gas constant and T the absolute temperature in K. The equilibrium constant, K_a is calculated from Ref. [11]:

$$\log K_a = -2.691122 \log T - 5.519265 \times 10^{-5} T + 1.848863 \times 10^{-7} T^2 + \frac{2001.6}{T} + 2.6899 \quad (4)$$

The fugacity of component i is given by definition as:

$$f_i = \phi_i Y_i P \quad (5)$$

where ϕ_i is the fugacity coefficient of component i, Y_i the mole fraction of component i, and P the total pressure. The fugacity coefficients are calculated by means of equations given by Mahfouz [12]. A drawback of Eq. (1) is that it is obviously not valid for very low ammonia concentrations since the first term diverges.

3. Model development

A heterogeneous one-dimensional model is developed for an adiabatic catalyst bed, and the following assumptions are made:

1. The bed is adiabatic and operating at steady-state conditions.
2. There is negligible heat-transfer resistance between the pellets and the gas [13].
3. Axial dispersion is negligible due to the high gas velocities [14].
4. The thermal and concentration gradients in the radial direction are negligible [15].
5. The pressure drop along the bed is negligible [16].
6. The specific heat of the reaction mixture is constant.

3.1. Material balance on the bulk gas

A molar differential balance for nitrogen in the catalyst bed gives:

$$\frac{dX}{dV} = \frac{\eta R_{NH_3}(X, T, P)}{2F_{N_2}^0} \quad (6)$$

where X is the fractional conversion of nitrogen, V the volume of catalyst bed in m^3, η the effectiveness factor, and $F_{N_2}^0$ the initial molar flow rate of nitrogen in kmol/h. The fractional conversion of nitrogen at any cross section of the bed can be written as:

$$X = \frac{\text{molar flow of } N_2 \text{ at inlet} - \text{molar flow of } N_2 \text{ at cross section}}{\text{molar flow of } N_2 \text{ at inlet}} \quad (7)$$

All mole fractions can be expressed in terms of the feed mole fractions and the fractional conversion of nitrogen.

3.2. Energy balance on the bulk gas

The energy balance for a differential element of the catalyst bed gives:

$$\frac{dT}{dV} = \frac{(-\Delta H_R)\eta R_{NH_3}(X, T, P)}{\dot{m} C_{p_{mix}}} \quad (8)$$

where ΔH_R is the heat of reaction in J/kmol of NH_3, $\dot{m}$ the total mass flow rate in kg/h, and $C_{p_{mix}}$ the specific heat of reacting gas mixture in J/(kg K). The heat of reaction has been calculated by using the empirical correlation presented by Strelzoff [8]. The molar specific heat of different components is calculated at the feed conditions from the equations given by Shah [15].

3.3. Effectiveness factor and the catalyst particle equations

The effect of diffusional resistance inside the catalyst which is important for the industrial catalyst particles (6–12 mm) is expressed in terms of the effectiveness factor, η. A rigorous approach for the treatment of the effectiveness factor problem is through formulating the diffusion-reaction equations, solving them, and calculating the effectiveness factor. The catalyst pellet equations are developed using the well-established assumptions presented by previous investigators [9–12].

A molar differential balance for component i inside the catalyst particle gives:

$$\frac{1}{r^2}\frac{d}{dr}(r^2 N_i) = \gamma_i \frac{R_{NH_3}(Y, T, P)}{1 - \varepsilon} \quad (9)$$

where N_i is the molar flux of the ith component in the r direction, ε the void fraction of the packed bed and is equal

to 0.46 [9], and γ_i the stoichiometric coefficient of the ith component in the reaction scheme given in Eq. (2). Following the ordinary convention, γ_i is positive for products, negative for reactants, and zero for inerts. Nitrogen, hydrogen, ammonia, methane, and argon have been designated as components 1, 2, 3, 4, and 5, respectively. The boundary conditions for Eq. (9) are:

$$\text{at } r = 0 \quad \frac{dY_i}{dr} = 0$$

$$\text{at } r = R_p \quad Y_i = Y_{ig} \tag{10}$$

where R_p is the radius of the sphere equivalent to an industrial sized particle and is equal to 2.85×10^{-3} m for industrial particles of 6–10 mm [9] and Y_{ig} the mole fraction at the surface of the catalyst particle and this will be assumed to be the same as in the gas phase.

Following some lengthy but straightforward manipulation of the equations, we end up with the following dimensionless equation for the catalyst pellets:

$$\frac{d^2Y_i}{d\omega^2} - \frac{1}{\gamma_i + Y_i}\left(\frac{dY_i}{d\omega}\right)^2 + \frac{2}{\omega}\frac{dY_i}{d\omega} = -\left(\frac{R_p^2}{CD_{ie}}\right)(\gamma_i + Y_i)\frac{R_{NH_3}(Y, T, P)}{1-\varepsilon} \tag{11}$$

and the boundary conditions in terms of ω are:

$$\text{at } \omega = 0 \quad \frac{dY_i}{d\omega} = 0$$

$$\text{at } \omega = 1 \quad Y_i = Y_{ig} \tag{12}$$

where $\omega = r/R_p$. The total concentration, C, is found from Ref. [10]:

$$C = \frac{\sum_{i=1}^{n} f_i}{R_G T} \tag{13}$$

where f_i is the fugacity of component i. The effective diffusion coefficient is calculated from the equation given by Wheeler [17] as:

$$D_{ie} = \tfrac{1}{2}\sigma D_i \tag{14}$$

where σ is the intraparticle porosity and D_i the bulk diffusion coefficient of component i. The intraparticle porosity is $\approx$0.52 according to Mahfouz [12]. The diffusion coefficients at 273 K and 101 325 Pa are given by Wilke equation as:

$$D_i^0 = \frac{1 - Y_{ig}}{\sum_{\substack{j=1 \\ j\neq 1}}^{n} (Y_{jg}/D_{ij}^0)} \tag{15}$$

The diffusion coefficients calculated from Eq. (15) are then corrected to the temperature and pressure at the surface of the catalyst pellet as follows [18]:

$$D_i = D_i^0 \left(\frac{T}{273}\right)^{1.75} \frac{101\,325}{P} \tag{16}$$

where P is in pascals.

The catalyst pellet Eq. (11) is a non-linear two-point boundary value differential equation. The equation was discretized by the global orthogonal collocation technique [19,20] and solved simultaneously with the material and energy balance equations (6) and (8) at each point along the length of the reactor to evaluate the effectiveness factor. The effectiveness factor was found with high accuracy via the summation formula, which requires knowledge of the solution at the interior collocation points and the boundary [19]. Needless to say, double precision used throughout all the computations.

4. Crossing reaction equilibrium

Nicol et al. [3] have shown by graphical methods that the optimization of heat exchange between different streams of an overall adiabatic system can result in higher conversions than the equilibrium conversion for a single adiabatic reactor. The method allows only internal heat exchange

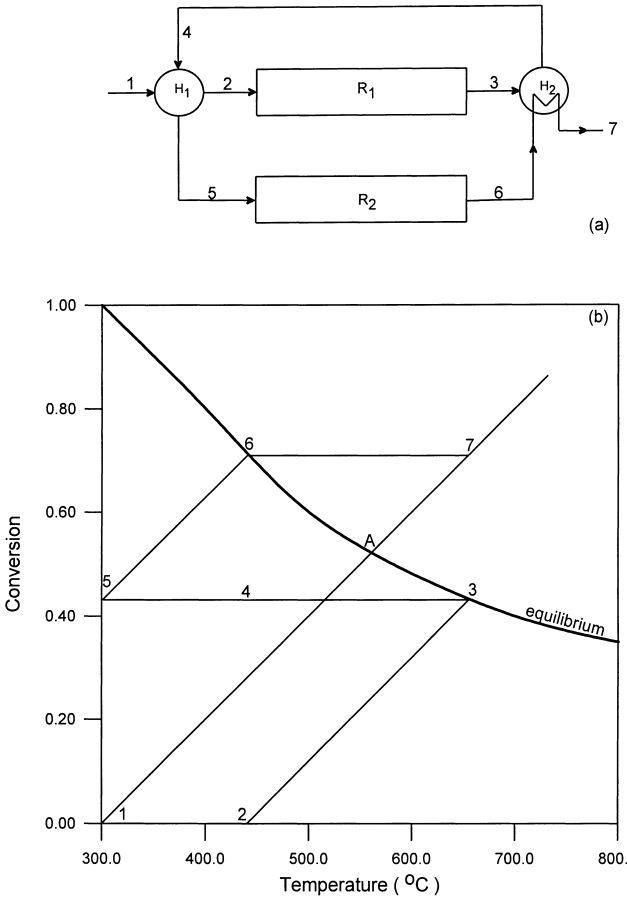

Fig. 1. (a) Schematic diagram of two reactors with two heat interchangers system, (b) crossing equilibrium in a two reactor system.

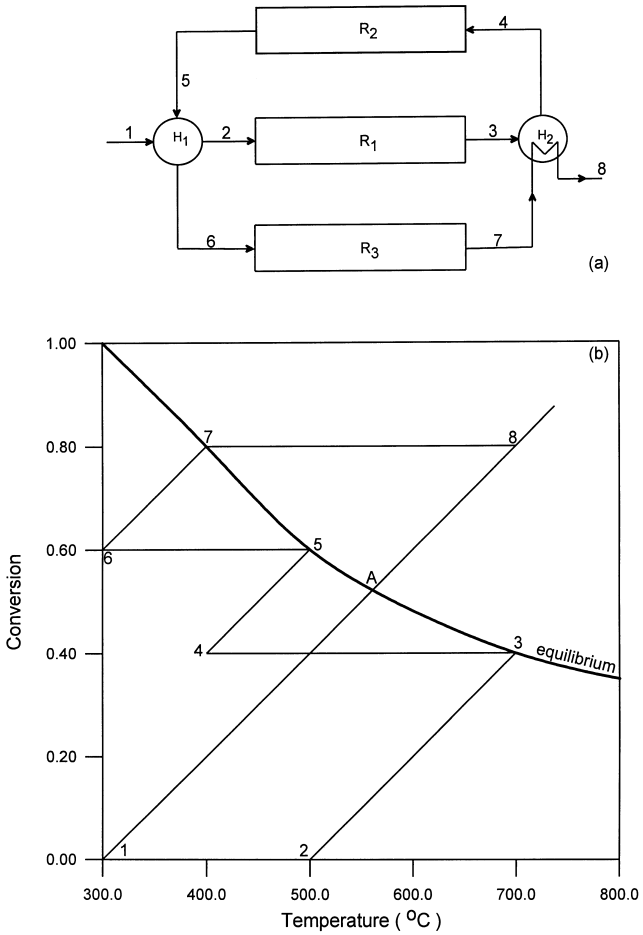

Fig. 2. (a) Schematic diagram of three reactors with two heat interchangers system, (b) crossing equilibrium in a three reactor system.

between streams, i.e. no source of external cooling or heating is required. A brief illustration of the idea is presented by considering two systems of reactors with heat interchangers. The main assumptions are as follows: the reaction is exothermic reversible and proceeds to the corresponding equilibrium conversion in all catalyst beds. The system is assumed to be an overall adiabatic. The specific heat of the reaction mixture is constant and the system is assumed at steady-state conditions.

4.1. Two reactors with two heat interchangers system

In this part, the theory of crossing the adiabatic reaction equilibrium value is illustrated by the graphical method. It is easy to check the energy balance and to match the heat loads between the set of cold and hot streams using this method.

Fig. 1a shows a schematic diagram of a reactor network system consisting of two reactors and two heat interchangers. A single adiabatic reactor having a feed temperature T_1 can achieve an equilibrium conversion of 0.520 at A as shown in Fig. 1b. This is the adiabatic equilibrium conversion. A higher optimal conversion (Z_7=0.710) can be achieved using two reactors with two heat interchangers system. This is done by preheating the feed from T_1 to T_2 countercurrently by the first heat interchanger (H_1). The first reactor (R_1) gives an equilibrium conversion of 0.432 at T_3. Stream 3 is cooled twice by countercurrent exchange of heat in the interchangers 2 (H_2) and 1 (H_1), respectively, i.e. from T_3 up to T_5. The second reactor (R_2) achieves an equilibrium conversion of 0.710 at T_6 and the reaction mixture is heated countercurrently in the second heat exchanger (H_2) to a final state at T_7. The interchange is theoretically correct because the temperature driving forces remain at zero. The temperature driving forces for this system are defined as follows:

$$\begin{aligned}\Delta T_1 &= T_4 - T_2\\ \Delta T_2 &= T_5 - T_1\\ \Delta T_3 &= T_3 - T_7\\ \Delta T_4 &= T_4 - T_6\end{aligned} \tag{17}$$

The correct energy balance is clearly shown in Fig. 2b. Line 1–2 (heat gained) equals to line 4–5 (heat lost) and line 3–4

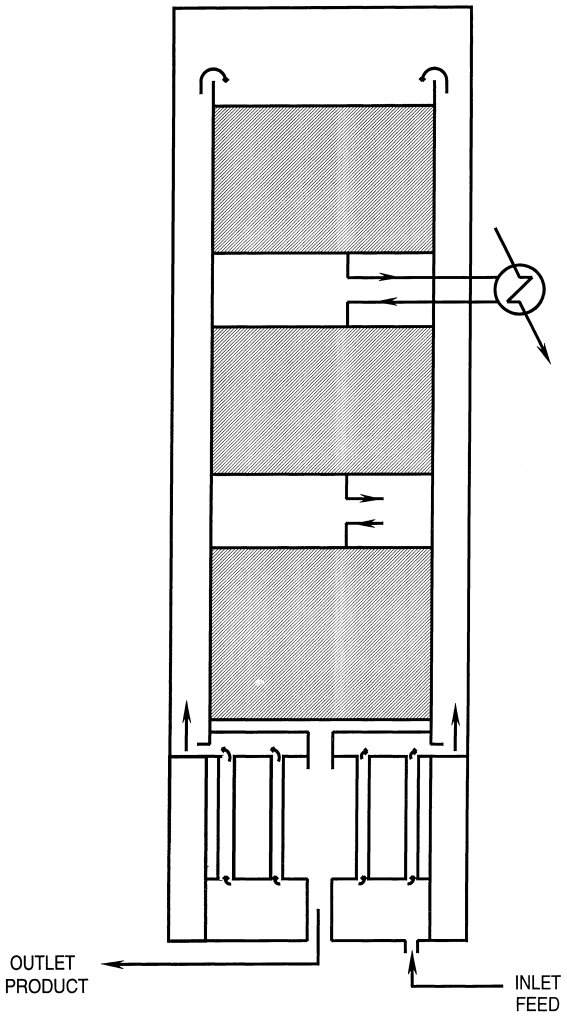

Fig. 3. Schematic diagram of a three-bed industrial ammonia reactor.

(heat lost) equals line 6–7 (heat gained). It is interesting that final state of the system at T_7 lies on the adiabat from the initial feed (T_1). The overall adiabatic condition of the system requires that the heat released by the chemical reaction in reactors 1 and 2 ($(T_3-T_2)+(T_6-T_5)$) equals the heat gained by the reaction mixture from the feed condition to the final state (T_1-T_7).

4.2. Three reactors with two heat interchangers system

A schematic diagram of a reactor network system consisting of three reactors and two heat interchangers is shown in Fig. 2a. The streams to the interchangers 1 and 2 are countercurrent and the temperature driving forces for heat transfer are:

$$\begin{aligned}\Delta T_1 &= T_5 - T_2\\ \Delta T_2 &= T_6 - T_1\\ \Delta T_3 &= T_3 - T_8\\ \Delta T_4 &= T_4 - T_7\end{aligned} \tag{18}$$

the system is theoretically possible because the temperature driving forces equal to zero as shown in Fig. 2b, i.e. there is no shortage of the energy supply. The final state of the system (T_8) lies on the adiabat from the initial feed condition (T_1) as indicative of the correct matching of the energy exchange in the system. The final conversion is Z_8=0.800 which is higher than the previous configuration. It can be seen from the above that addition of further reactors has significant effect on the improvement of the final conversion.

5. Results and discussion

5.1. Validation of the mathematical model

Industrial data from a reactor having three adiabatic beds with Montecatini Edison catalyst and interstage cooling [10] are used to validate the heterogeneous model. A simplified schematic diagram of the industrial reactor is given in Fig. 3. Summary of the comparison between the experimental data and the simulation results is given in Table 1.

It clearly shown that the heterogeneous model simulated the industrial reactor well. The details of the validation of the heterogeneous model is given elsewhere [7].

5.2. Applications

In this section, we apply the internal heat exchange theory as described above to different configurations of reactor network systems.

5.2.1. Two reactors with two heat interchangers configuration

Each catalyst bed of the industrial reactor is treated as an overall adiabatic system. Each system is a reactor network consisting of two reactors and two heat interchangers as shown in Fig. 1. Three of these reactor network systems form the process under investigation. The volumes of the catalyst of the first, second and third system are 4.75, 7.20 and 7.80 m^3, respectively. The systems are connected in series and the feed temperature to each system is considered

Table 1
Comparison between experimental data and simulation results (total feed flow, 242 160 ($N m^3$)/h; pressure, 22.89945 MPa)

	Composition (mol%)					Temperature (°C)	Conversion
	N_2	H_2	NH_3	CH_4	Ar		
Bed_1: volume of the catalyst, 4.75 m^3							
Inlet							
	22.19	67.03	2.76	5.46	2.56	385.000	0.0000
Outlet							
Experimental	20.10	61.00	10.50	5.70	2.70	507.000	0.1578
Heterogeneous model	20.06	60.67	10.64	5.88	2.76	506.470	0.1604
Bed_2: volume of the catalyst, 7.20 m^3							
Inlet							
Experimental	20.10	61.00	10.50	5.70	2.70	433.000	0.1578
Heterogeneous model	20.06	60.67	10.64	5.88	2.76	433.000	0.1604
Outlet							
Experimental	18.20	57.10	15.90	6.10	2.70	502.000	0.2555
Heterogeneous model	18.69	56.60	15.68	6.15	2.88	504.148	0.2517
Bed_3: volume of the catalyst, 7.80 m^3							
Inlet							
Experimental	18.20	57.10	15.90	6.10	2.70	415.000	0.2555
Heterogeneous model	18.69	56.60	15.68	6.15	2.88	415.000	0.2517
Outlet							
Experimental	17.80	53.90	19.10	6.30	2.90	455.000	0.3091
Heterogeneous model	17.71	53.67	19.31	6.34	2.97	462.105	0.3126

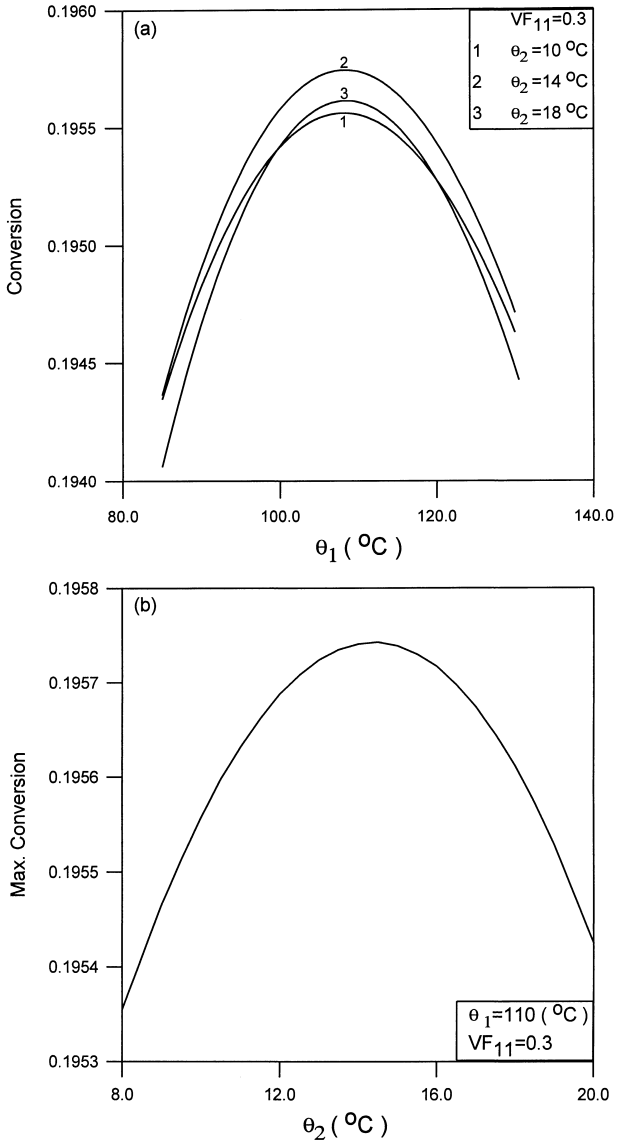

Fig. 4. Two reactors with two heat interchangers configuration: (a) plots of conversion as function of θ_1 for different values of θ_2 and VF_{11}=0.3; (b) locus of maxima shown in (a) at θ_1=110°C and VF_{11}=0.3.

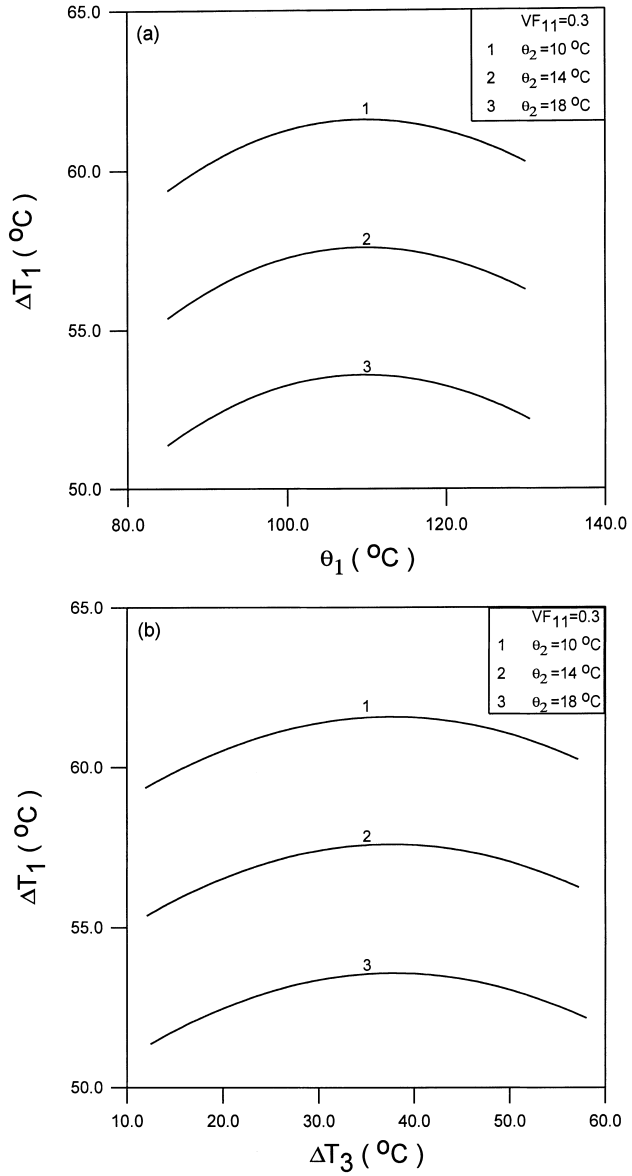

Fig. 5. Two reactors with two heat interchangers configuration: ΔT_1 as function of (a) θ_1; and (b) ΔT_3 for different values of θ_2 and VF_{11}=0.3.

to be the same as the industrial reactor as shown in Table 1 (385, 433, 415°C). The numbers 1,2,3...etc. are used to denote the state conditions of each system. The assumption of constant specific heat of the reaction mixture gives:

$$\Delta T_1 = \Delta T_2, \qquad \Delta T_3 = \Delta T_4 \tag{19}$$

hence, the cold and warm fluid ranges can be written as:

$$\theta_1 = T_2 - T_1 = T_4 - T_5 \tag{20}$$

$$\theta_2 = T_3 - T_4 = T_7 - T_6 \tag{21}$$

For the system to be practically possible, the temperature driving forces must satisfy:

$$\Delta T_i > 0, \quad i = 1 - 4 \tag{22}$$

Table 2
Comparison between simulation results and optimal sequence based on the system of two reactors with two heat interchangers

	Conversion	Increase (%)
Volume of catalyst, 4.75 m^3		
Industrial reactor (simulation, Bed_1)	0.1604	
System 1	0.1955	21.88
Volume of catalyst, 7.20 m^3		
Industrial reactor (simulation, Bed_2)	0.2517	
System 2	0.2874	14.18
Volume of catalyst, 7.80 m^3		
Industrial reactor (simulation, Bed_3)	0.3126	
System 3	0.3438	9.98

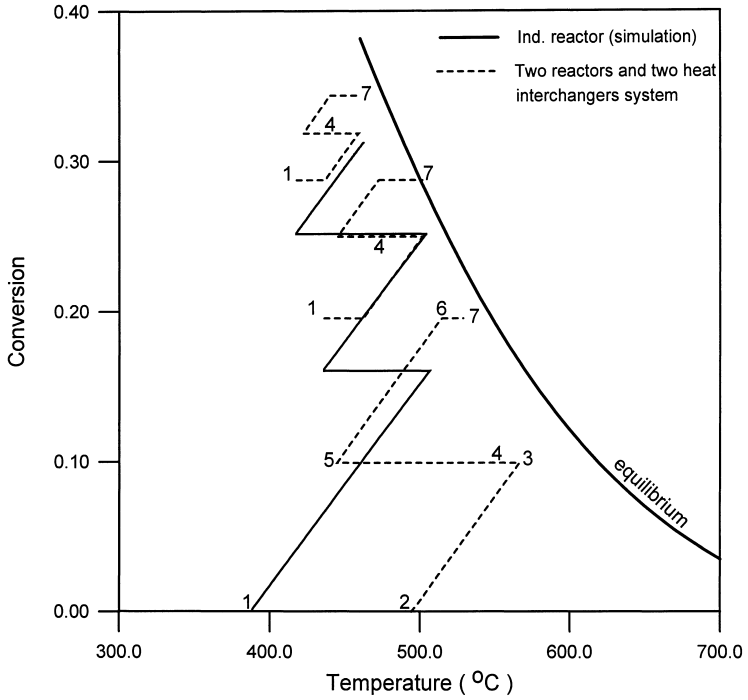

Fig. 6. Comparison of the conversion obtained by the simulation of the industrial reactor (Bed_1=4.75 m^3, Bed_2=7.20 m^3, Bed_3=7.80 m^3) and the optimal sequence policy using two reactors with two heat interchangers systems (VF_{11}=0.3, VF_{21}=0.5, VF_{31}=0.5).

In order to obtain a feasible region of positive temperature driving forces for all systems, the key parameters should be identified. Here, we have considered the following main parameters: the volume fraction of the catalyst bed (VF_{ij}), θ_1 and θ_2. To simplify the problem, the three-parameter space is reduced to two-parameter space by considering the search at constant volume fractions of the catalyst bed. This approach gives feasible regions at different values of volume fractions

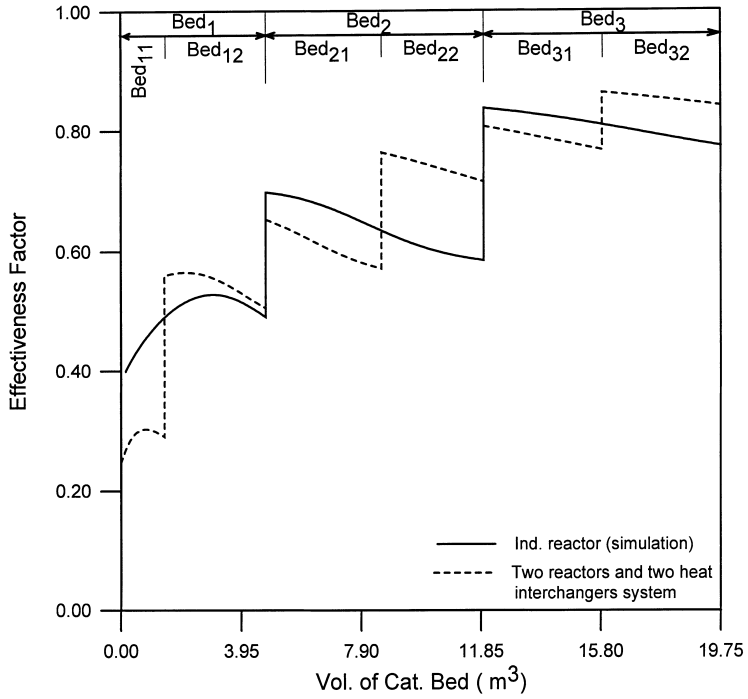

Fig. 7. Comparison of the effectiveness factor obtained by the simulation of the industrial reactor (Bed_1=4.75 m^3, Bed_2=7.20 m^3, Bed_3=7.80 m^3) and the optimal sequence policy using two reactors with two heat interchangers systems (VF_{11}=0.3, VF_{21}=0.5, VF_{31}=0.5).

of the catalyst bed. Initial guesses are required to find the fluid ranges (θ_1, θ_2) which give the positive temperature driving forces. These initial guesses are obtained by iteration to satisfy the condition of zero driving forces ($\Delta T_i=0$). With these initial guesses, trial and error is used as follows: The volume fraction is fixed in the interval $0.0<VF_{ij}<1.0$. The feed temperature (T_1) is known. The temperature ranges θ_1 and θ_2 are assumed. The exit temperature (T_2) from the first heat interchanger is obtained from Eq. (20) and T_3 is calculated by solving the model equations of the first reactor (R_1). Hence, T_4 and T_5 are obtained from equations (21) and (20), respectively, T_6 is calculated by solving the model equations of the second reactor (R_2) and T_7 is obtained from Eq. (21). Then, the temperature driving forces are calculated using Eq. (17) and the condition of positive driving forces is checked by Eq. (22).

The survey of all feasible regions to obtain the maximum conversion for each system and the optimum configuration of the integrated systems is a complex problem. The approach used in this study makes use of decomposition in optimization in a very simple manner. Each system is analyzed individually to give the optimal exit composition which is used as a feed to the next system. Despite the rough results obtained by this approach it reduces the number of permutations significantly in this preliminary study.

As an illustration, we will present a sample of suboptimal solutions obtained using our adopted optimization approach. We have chosen the first system for this example. Fig. 4a shows plots of conversion versus θ_1 for different values of θ_2 and constant volume fraction ($VF_{11}=0.3$). The volume fraction is based on the total volume of the catalyst used in the system, in this case 4.75 m^3. It is clearly shown that the conversion has an extremum with respect to θ_1. The maxima are at an average value of $\theta_1=110^\circ C$. The locus of the maximum conversion is obtained by plotting the maximum values in Fig. 4a versus θ_2 at $\theta_1=110^\circ C$ as Fig. 4b shows. Hence, the optimal exit conversion is obtained from Fig. 4b. It is clear that the optimization involves repeated use of a one-dimensional search. A computer program is developed based on the Fibonacci search method, which is an efficient region elimination method for a one-dimensional search. The program includes a routine which is used to find the final optimal sequence policy from the possible suboptimal solutions.

Fig. 5a and b shows that the driving force ΔT_1 has an optimal value with respect to both θ_1 and ΔT_3 and decreases with the increase of θ_2.

Fig. 6 shows the final optimal sequence. It is clearly shown that the exit conversions from each system obtained by this policy are much higher than the simulation results of the industrial reactor. A significant increase of 9.98% of the final conversion is achieved as shown in Table 2.

The intraparticle mass transfer resistance affects the actual rate of reaction and the conversion. Fig. 7 shows the effectiveness factor profiles along the reactor length. It is clearly shown that the optimal internal heat exchange

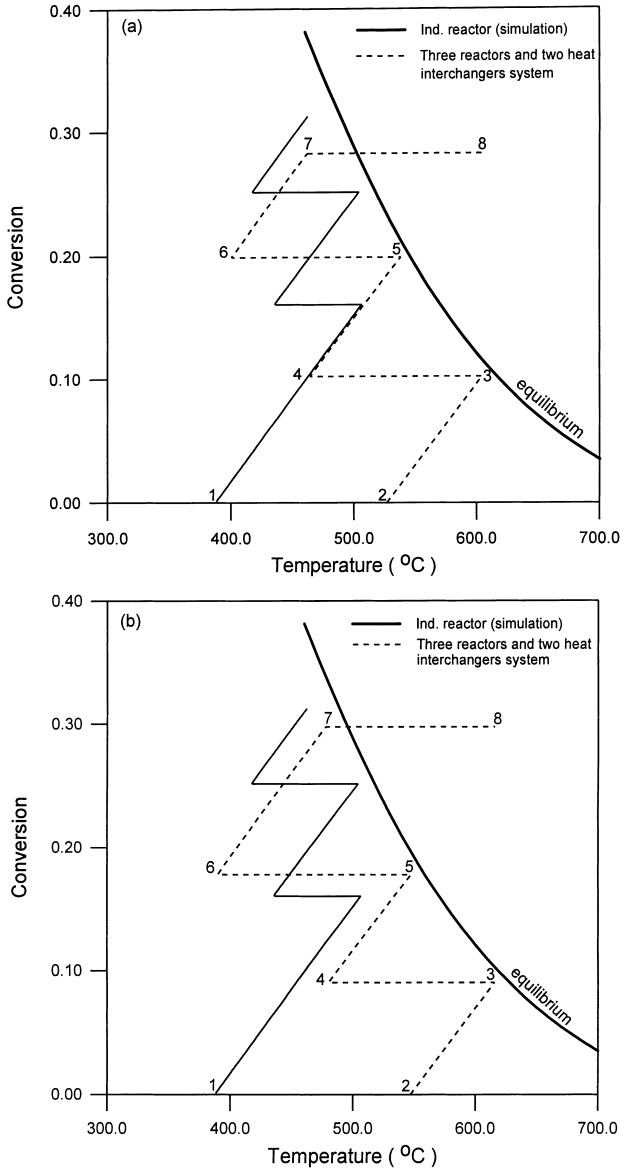

Fig. 8. Comparison of the conversion obtained by the simulation of the industrial reactor ($Bed_1=4.75\,m^3$, $Bed_2=7.20\,m^3$, $Bed_3=7.80\,m^3$) and the optimal sequence policy using three reactors with two heat interchangers system: (a) $Bed_1=4.75\,m^3$, $Bed_2=7.20\,m^3$, $Bed_3=7.80\,m^3$; and (b) $Bed_1=3.00\,m^3$, $Bed_2=4.30$, $Bed_3=12.45\,m^3$.

policy has a profound effect on the effectiveness factor. The increase of the temperature increases the intrinsic rate of reaction as well as the effective diffusivities. The increase of the rate of the reaction and the effective diffusivities have conflicting effects on the effectiveness factor. The increase of the intrinsic rate of reaction tends to decrease the effectiveness factor and the increase of the effective diffusivities tends to increase the effectiveness factor. The effectiveness factor profiles presented in Fig. 7 can be explained by considering the interaction of these factors. Elnashaie et al. [21] have pointed out the effect of the interaction of these factors on the effectiveness factor behaviour.

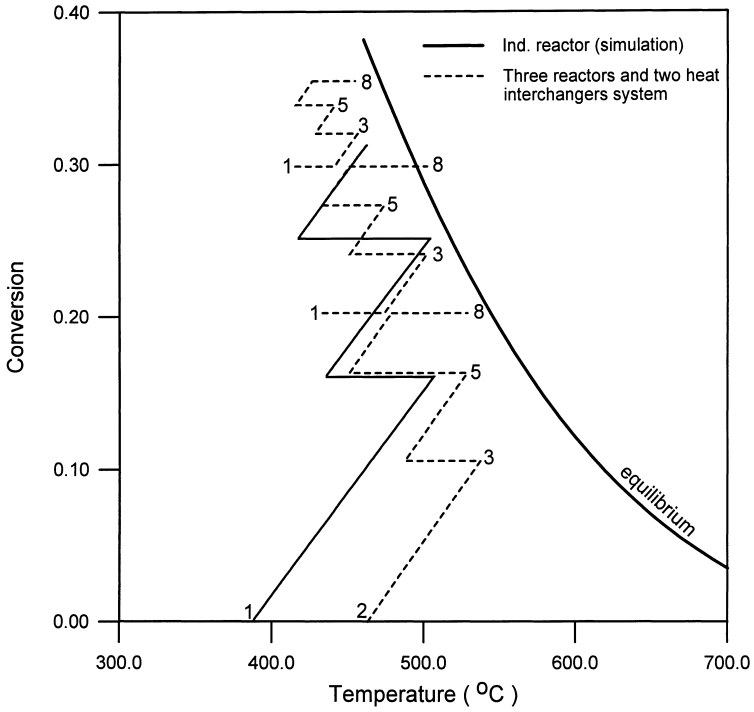

Fig. 9. Comparison of the conversion obtained by the simulation of the industrial reactor (Bed_1=4.75 m^3, Bed_2=7.20 m^3, Bed_3=7.80 m^3) and the optimal sequence policy using three reactors with two heat interchangers systems (VF_{1j}=1.5833 m^3, VF_{2j}=2.4000 m^3, VF_{3j}=2.6000 m^3).

5.2.2. Three reactors with two heat interchangers configuration

In this part, the effect of addition of a reactor to the previous configuration (two reactors with interchangers) is investigated. This type of configuration is shown in Fig. 2. Two cases are considered. The first case considers the industrial reactor as a single reactor network system while the second case uses three systems as in Section 5.2.1.

In the first case, the feed temperature to the second and third reactor is determined by optimal calculations, i.e. there is no external interstage cooling. Fig. 8a shows the optimal sequence policy when the volume of the catalyst bed in each reactor is same as the industrial reactor as shown in Table 1 (4.75, 7.2, 7.8 m^3). An overall conversion of 0.2828 is achieved. The effect of distribution of the catalyst among the reactors is shown in Fig. 8b. An overall conversion of 0.2977 is obtained by the optimal sequence policy when the volumes of the catalyst in the first, second and third reactors are 3.0, 4.3 and 12.8 m^3, respectively. The distribution of the catalyst among the reactors is an important optimization factor which may lead to the improvement of the overall conversion. The overall conversions achieved by these systems are comparative to the industrial reactor. Despite the fact that the overall conversion obtained by these systems is less than the industrial reactor, the heat load decreases because no external quenching is used.

In the second case, we have three systems with nine reactors. The systems are connected in series and the feed temperatures to the systems are taken as the feed temperatures to the catalyst beds of the industrial reactor. To simplify the problem, the volume of the catalyst in each system is equally divided among the reactors, i.e. the volume of catalyst is constant in each reactor. Hence, the key parameters are θ_1 and θ_2. The calculation procedure used for the previous configuration is also applicable in this case, however, there are more combinations.

Fig. 9 shows the results of maximizing the conversion by the optimal sequence policy. A substantial improvement of 13.37% in the final conversion is obtained. Comparison between the optimal exit conversion from each system and the simulation results of the industrial reactor are presented in Table 3.

Fig. 10 shows the effectiveness factor profiles along the length of the reactor. The diffusional resistance decreases in the second and the third systems compared to the industrial

Table 3
Comparison between simulation results and optimal sequence based on the system of three reactors with two heat interchangers

	Conversion	Increase (%)
Volume of catalyst, 4.75 m^3		
Industrial reactor (simulation, Bed_1)	0.1604	
System 1	0.2024	26.18
Volume of catalyst, 7.20 m^3		
Industrial reactor (simulation, Bed_2)	0.2517	
System 2	0.2986	18.63
Volume of catalyst, 7.80 m^3		
Industrial reactor (simulation, Bed_3)	0.3126	
System 3	0.3544	13.37

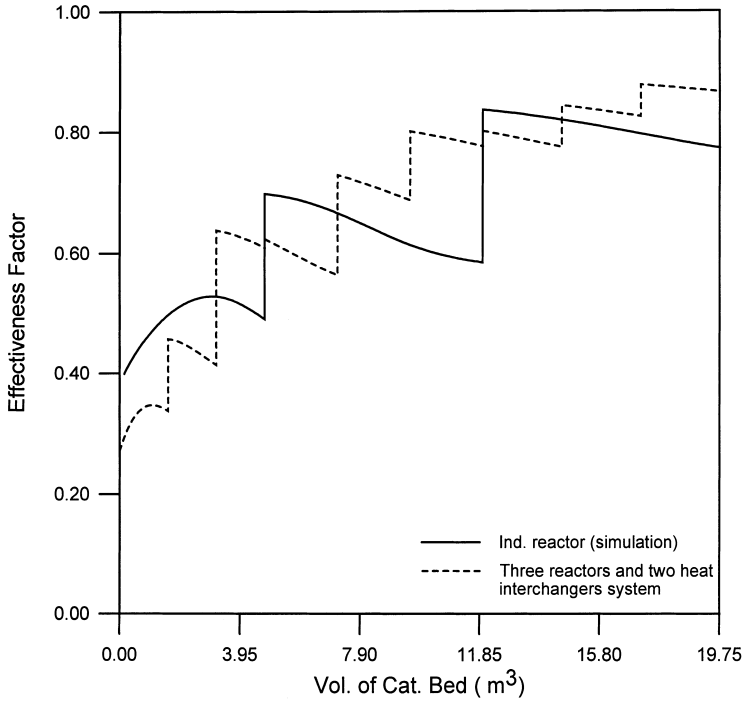

Fig. 10. Comparison of the effectiveness factor obtained by the simulation of the industrial reactor (Bed_1=4.75 m^3, Bed_2=7.20 m^3, Bed_3=7.80 m^3) and the optimal sequence policy using three reactors with two heat interchangers systems (VF_{1j}=1.5833 m^3, VF_{2j}=2.4000 m^3, VF_{3j}=2.6000 m^3).

reactor (second and third beds) and this could be one of the reasons for the enhancement of the overall conversion.

6. Conclusions

In the present paper, the concept of crossing the adiabatic reaction equilibrium values using internal heat exchange was applied to an industrial adiabatic ammonia reactor. The investigation was carried out using two simple configurations for energy optimization: two or three reactors with two heat interchangers. A rigorous mathematical model was used to simulate the ammonia reactors. The results clearly show that a significant improvement in ammonia conversion is achieved using these configurations. The energy optimization and integration can play an important role in the performance of ammonia reactors. This study also show that the traditional methods of quenching operations in the ammonia industry should be re-addressed.

And finally, although we did not include cost factors or implemented sophisticated optimization techniques, the reported results are very promising in view of the fresh challenges in application and research of heat integration and optimization in the ammonia industry.

List of symbols

C	total concentration, kmol/m^3
$C_{p_{mix}}$	specific heat of reacting gas mixture, J/(kg K)
D_i	diffusion coefficient of component i, m^2/h
D_i^0	diffusion coefficient of component i at 273 K and 101 325 Pa, m^2/h
D_{ij}^0	diffusion coefficient of component j in component i, m^2/h
D_{ie}	effective diffusion coefficient of component i, m^2/h
E_2	activation energy for ammonia decomposition, J/kmol
f_i	fugacity of component i, Pa
$F_{N_2}^0$	molar flow rate of nitrogen at reactor inlet, kmol/h
ΔH_R	heat of reaction, J/kmol of NH_3
k_2	velocity constant of reverse reaction, kmol/(h m^3)
k_{20}	frequency factor in Arrhenius equation for k_2
K_a	equilibrium constant of reaction 2
$\dot{m}$	total mass flow rate, kg/h
N_i	molar flux of component i in r direction
P	total pressure, Pa
r	radial co-ordinate of spherical catalyst particle
R_{NH_3}	rate of ammonia formation, kmol of NH_3/(h m^3 of catalyst bed)
R_G	universal gas constant, J/kmol K
R_p	radius of spherical particle, m
T	temperature, K
V	volume of catalyst bed, m^3
VF_{ij}	volume fraction of catalyst bed j in system i
X	conversion based on nitrogen

Y_i mole fraction of component i
Y_{ig} mole fraction of component i in gas (bulk phase)

Greek symbols
α kinetic parameter
γ_i stoichiometric coefficient of component i
ϕ_i fugacity coefficient of component i
η effectiveness factor
ε void fraction of packed bed
ω dimensionless radial co-ordinate of a spherical particle
σ intraparticle porosity

Acknowledgements

The author wishes to express his thanks to Dr. D.K. Kuwornoo for his help in editing this paper.

References

[1] Z. Ziaka, V. Manousiouthakis, Best achievable isomerization reaction conversion in a membrane reactor, Ind. Eng. Chem. Res. 37 (1998) 3551.
[2] T. Tsotsis, A. Champagnie, S. Vasileiadis, Z. Ziaka, R. Minet, The enhancement of reaction yield through the use of high temperature membrane reactors, Sep. Sci. Technol. 28 (1993) 397.
[3] W. Nicol, D. Hildebrandt, D. Glasser, Crossing reaction equilibrium in an adiabatic reactor system, Dev. Chem. Eng. Mineral Process 6 (1998) 41.
[4] R. Aris, Studies in optimization. I: the optimum design of adiabatic reactors with several beds, Chem. Eng. Sci. 12 (1960a) 243.
[5] R. Aris, Studies in optimization. II: optimum temperature gradients in tubular reactors, Chem. Eng. Sci. 13 (1960) b) 75.
[6] P.G. Bhandarkar, G. Narasimhan, An algorithm for optimization of adiabatic reactor sequence with cold shot cooling, Ind. Eng. Chem. Process Des. Dev. 8 (1969) 143.
[7] S.S. Elnashaie, M.E. Abashar, A.S. Al-Ubaid, Simulation and optimization of an industrial ammonia reactor, Ind. Eng. Chem. Res. 27 (1988) 2015.
[8] S. Strelzoff, Technology and Manufacture of Ammonia, Wiley: New York, 1981.
[9] D.C. Dyson, J.M. Simon, A kinetic expression with diffusion correction for ammonia synthesis on industrial catalyst, Ind. Eng. Chem. Fundam. 7 (1968) 605.
[10] C.P.P. Singh, D.N. Saraf, Simulation of ammonia synthesis reactors, Ind. Eng. Chem. Process Des. Dev. 18 (1979) 364.
[11] L.D. Gaines, Ammonia synthesis loop variables investigated by steady-state simulation, Chem. Eng. Sci. 34 (1979) 37.
[12] A.T. Mahfouz, Steady-state modeling and simulation of industrial ammonia synthesis reactor, Ph.D. Dissertation, The University of Cairo, Egypt, 1985.
[13] C.A. Vancini, Synthesis of ammonia, The MacMillan Press, London, 1971.
[14] K.V. Reddy, A. Husain, Modeling and simulation of an ammonia synthesis loop, Ind. Eng. Chem. Process Des. Dev. 21 (1982) 359.
[15] M.J. Shah, Control simulation of ammonia production, Ind. Eng. Chem. 59 (1967) 72.
[16] R.F. Baddour, P.L.T. Brain, B.A. Logeais, P.J. Eymery, Steady-state simulation of an ammonia synthesis converter, Chem. Eng. Sci. 20 (1965) 281.
[17] A. Wheeler, Catalysis, in: P.H. Emmett (Ed.), Reinhold, New York, 1955.
[18] C.J. Geankoplis, Transport Processes and Unit Operations, Allyn and Bacon, Inc., 1978.
[19] J. Villadsen, M.L. Michelsen, Solution of Differential Equation Models by Polynomial Approximation, Prentice-Hall, Inc. Englewood Cliffs, 1978.
[20] B.A. Finlayson, Nonlinear Analysis in Chemical Engineering, McGraw-Hill Inc., 1980.
[21] S.S.E.H. Elnashaie, M.E.E. Abashar, A.S. Al-Ubaid, Non-monotonic behavior of the effectiveness factor along a catalyst bed, Chem. Eng. Sci. 44 (1989) 1581.